17th World Conference on Earthquake Engineering, 17WCEE
Sendai, Japan - September 13th to 18th 2020

The Ruff and Kanamori Diagram Reproduced with a Spring-block Model

A. Muñoz-Diosdado[(1)], J. Perez-Oregon[(2)], F. Angulo Brown[(2)]

[(1)] *Departamento de Ciencias Básicas, Unidad Profesional Interdisciplinaria de Biotecnología, Instituto Politécnico Nacional, Mexico City, Mexico, amunozdiosdado@gmail.com*
[(2)] *Departamento de Física, Escuela Superior de Física y Matemáticas, Instituto Politécnico Nacional, Mexico City, Mexico, jnnfr.po@gmail.com, angulo@esfm.ipn.mx*
…

Abstract

The distribution of the number of events in terms of their sizes in actual seismicity, which has the form of a power law, is indicative of the self-organized critical nature this process. This law is of the Gutenberg-Richter type ($log\dot{N} = a - bM$). In the Olami, Feder and Christensen (OFC) self-organized critical (SOC) model there is a negative correlation between the b-value and the γ elastic ratio of the springs linking the blocks of this system. As this γ elastic ratio can be related with an aging effect, it is possible to incorporate a dependence on time of some features of the SOC system. Thus, we can describe aging effects over possible SOC systems such as actual subduction zones. We can also propose the way to incorporate the relative velocity between plates in a SOC model. With these ideas we can qualitatively reproduce the so-called Ruff-Kanamori (RF) diagram for subduction zones around the world.

Many researchers have proposed numerical models that look forward to reproduce some important features of actual seismicity by using suitable simplified SOC models capturing the main dynamical characteristics of earthquakes. One of the most used SOC models to emulate the interaction between tectonic plates is the 2D spring-block model proposed by OFC. This model produces well-behaved Gutenberg-Richter relationships for the statistics of the number of earthquakes in terms of their magnitudes. However, the SOC nature of the seismicity would be reinforced if other of its important characteristics were also reproduced by the mentioned SOC models.

In this work we have extended the application of the OFC SOC model to other important global features of actual seismicity. One of our goals was to reproduce the so-called Ruff-Kanamori (RK) diagram, which relates the magnitude (M_w) of the largest characteristic earthquake of a given subduction zone with the convergence rate between the down going and upper plates and with the age of the subducted plate. We obtained the synthetic version of a RK-type diagram where we used the γ elastic ratio of the OFC SOC model as an analogue of the age of the corresponding tectonic plates. On the other hand, the convergence rate in the RK diagram was emulated by means of the adding of a new rule to the set of rules of the OFC model. The magnitude of synthetic OFC earthquakes was calculated by means of $M_{syn} = \ln(n)$, being n the number of relaxed blocks in each event. Interestingly, we obtained that M_{syn} depends on the synthetic velocity and the synthetic age.

Keywords: self-organized criticality, spring-block, convergence rate, age of subducted plate, Ruff-Kanamori diagram

17th World Conference on Earthquake Engineering, 17WCEE
Sendai, Japan - September 13th to 18th 2020

1. Introduction

Any model that aspires to represent the actual seismicity needs at least to reproduce the statistical behavior enclosed in the Gutenberg-Richter [GR] law [1,2]:

$$\log \dot{N} = a - bM, \tag{1}$$

where a and b are the GR parameters; $\dot{N}$ is the number of earthquakes per year with magnitude larger than M. The a-value is a measure of the regional level of seismicity and the b-value is the slope of the straight line represented by Eq. (1). However, it is desirable that the model embraces some other important features of seismicity. A well-established feature of actual seismicity is that each subduction zone around the world is characterized by its own largest earthquake. Ruff and Kanamori (RK) [3] introduced strength of coupling as measured by M_w as an important physical feature of subduction zones, and found that both Benioff zone geometry and strength of coupling are significantly correlated to two variables: age of subducting oceanic lithosphere and plate convergence rate. Here, we qualitatively try to reproduce the actual behavior of seismicity expressed in Fig. 2 of RK [3] and we will call it Ruff-Kanamori diagram. On the other hand, we also reproduce Fig. 11.34 of Lay and Wallace (LW) [4] which is a modified form of the RK diagram.

2. OFC model

The emulation of these graphs is accomplished by using the OFC spring-block SOC model [5, 6]. The OFC spring-block model consists of a two-dimensional dynamic system made by a network of blocks interconnected by springs. The blocks that are not on the network boundary have four neighbors. Each block is also joined by a spring to an upper rigid plate which moves with a small and constant speed (see Fig. 1 of [5]). A block will slip when the force over it is larger than some threshold value F_{th} (the maximal static friction). The forces will redistribute in its nearby neighbors due to the movement of the block, leading to a chain reaction made up of more slidings. The dynamics of the OFC model was accomplished by OFC [5, 6] by using a cellular automaton. They expressed the total force exerted by the springs on a given block (i,j) and after a local slip at the position (i,j), calculated the force redistribution in the four neighbors, and the increase in strength in the closest neighbors is given by [5,6],

$$\delta \mathrm{F}_{\mathrm{i}\pm1,\mathrm{j}} = \frac{K_1}{2K_1 + 2K_2 + K_L} F_{i,j} = \gamma_1 F_{i,j};$$

$$\delta \mathrm{F}_{\mathrm{i,j}\pm1} = \frac{K_2}{2K_1 + 2K_2 + K_L} F_{i,j} = \gamma_2 F_{i,j}; \tag{2}$$

where γ_1 and γ_2 are the elastic ratios, the K's are the springs constants. These elastic ratios can take values in the interval $0 < \gamma < 0.25$; yet, the values of the parameter b of the G-R law that are similar to real seismicity b-values are only obtained for γ around 0.2 [5-9]. For the isotropic case, $K_1 = K_2 = K_L$ ($\gamma_1 = \gamma_2 = \gamma$). The size of a synthetic earthquake is the number n of relaxed blocks and we can define its magnitude as a function of n, for instance, $M = log_x n$, where x is a convenient base of the logarithm. The evolution rules of the cellular automaton are the following:

1) Initialize all the sites of the lattice with random values between zero and a force threshold F_{th}.
2) For all $F_{i,j} \geq F_{th}$, redistribute the force in the neighbors of $F_{i,j}$ according to the rule

$$\mathrm{F_{n,n}} \rightarrow \mathrm{F_{n,n}} + \gamma \mathrm{F_{i,j}},$$
$$F_{i,j} \rightarrow 0,$$

where $\mathrm{F_{n,n}}$ are the forces of the neighbor blocks of the cell $\mathrm{F_{i,j}}$ that relaxed.
3) Step 2 must be repeated until the earthquake has completely evolved.

4) Localize the block with the largest force, $F_{\max}$. Add $F_{th} - F_{\max}$ to all sites (global perturbation). Coming back to step 2 until the number of events (synthetic earthquakes) is completed.
4') This step will be used by us only in the case that one wishes to emulate an increase in the relative velocity between the two rigid plates involved in the OFC model: Add $\Delta F > F_{th} - F_{\max}$ as a global perturbation just for once. Coming back to step 2 until the number of events is completed.

3. Results

According to RK [3] there is considerable variation between subduction zones in regard to the largest characteristic earthquake within each zone. Assuming that coupling between downgoing and upper plates is directly related to the largest characteristic earthquake size, they have tested for correlations between variation in coupling and other physical features of subduction zones. RK reported the location of characteristic largest earthquakes for 21 subduction zones around the world with their M_w, depth, rupture length, age of subduction oceanic lithosphere and convergence rate.

In their 1992 paper OFC establish that when the two rigid plates move one with respect to the other the total force on each block increases uniformly with a rate proportional to $K_L V$, where V is the relative velocity between the two rigid plates, and K_L is the elastic constant of the vertical springs, until one site reaches the threshold value and the process of relaxation begins. For qualitatively reproducing the mentioned RK diagram we use the same procedure of OFC, which we also have used in two recent papers [10, 11]. Although Olami et al. suggested the way to include the relative velocity between the two plates of their model, this idea have not been used to emulate certain features of tectonic environments as the subduction zones involved in the RK diagram. We have proposed an additional evolution rule to the OFC SOC model (see rule 4'). In Table 1, first column corresponds to ages of the subducting lithosphere and in Table 2, first column corresponds to convergence rates, both included in the RK diagram (Fig. 2 and Table 1 of [3]). The ages go from 20 Myr (Colombia and South Chile) to 150 Myr (Marianas and Izu-Bonin) and the relative velocities between plates go from 2.0 cm/yr (Caribbean and Scotia Arc) to 11.1 cm/yr (South Chile). We run the OFC model by putting $F_{th} = 4$, then if any block reaches this value after the initialization (rule 1) then the block with the largest force, $F_{\max}$, is located and a quantity $F_{th} - F_{\max}$ is added to all sites and coming back to step 2 of Section 2, until the number of events is completed. To emulate an increase in the relative velocity between the two plates we proceed according to rule 4' of Section 2. Pardo and Suárez [12] reported that the relative velocity between the Cocos and the North American plates along of the Mexican Pacific trench has an increasing value from the Colima-Jalisco zone until the Chiapas zone. The number of earthquakes of any magnitude per year along this same section of the Mexican trench has also a crescent behavior. This fact suggests that the OFC proposal that consists in the way to increase the total force in each block as proportional to the product $K_L V$, is reasonable; that is, the bigger the relative velocity V the bigger $F_{i,j}$ on each block according to Hooke's law, and therefore the probability that one or many blocks reach or exceed F_{th} increases. On the other hand, in Perez-Oregon et al. [10, 11] was suggested that the elastic ratio γ (see Eq. (2)) can be associated to an aging effect.

In second column of Table 1A we list a set of γ-values emulating the aging effect in the OFC model; that is, bigger values for young tectonic plates and smaller values for ancient tectonic plates. The correspondence between age of tectonic plates and the γ-values was proposed assigning $\gamma = 0.20$ to the youngest plate and $\gamma = 0.07$ to the oldest one and following an arbitrary rule, where for each increase of 10 Myr in the age of the plates a decrease of 0.01 in the γ-value is taken. However, for the gamma-elastic ratio in the interval [0.07, 0.20] the linear behavior with respect to the slope b is much better than out of this interval. The step between gamma-values in this plot is of 0.01 corresponding to 14 subintervals between [0.07, 0.20]. On the other hand, in the RK diagram (Fig. 2) the temporal scale goes from [0, 160] Myr spaced each 20 Myr (reporting largest earthquakes mainly in the interval [20, 150] Myr). Then, mainly for practical reasons we mapped the 14 gamma-subintervals to 14 age-subintervals resulting in Table 1A (in reference [11] this was explained with more detail). In second column of Table 1B we list a set of values for the synthetic relative velocity between the two plates of the OFC model. This list was elaborated by mapping the increments of actual velocity values (first column of Table 1B) which are of 1 cm/yr into synthetic

increments of 0.25. According to the OFC model the increase in the relative velocity between plates produces an increment in the total force on each block (i, j), then we propose to emulate the increments in the relative velocity by assigning force increments ΔF larger than $F_{th} - F_{max}$ when making the global perturbation; that is, instead of just adding $F_{th} - F_{max}$ in this step add a larger quantity guaranteeing that more blocks reach a value $F_{i,j}$ larger than F_{th}. In this way, according to ΔF increases, more and more blocks are perturbed since the beginning of the runs. We find that ΔF in the interval [0,3], with increments of 0.25 works reasonably to emulate the increments of actual relative velocity.

Table 1 – A. Left column gives the age range reported in the RK-diagram. Right column gives the γ-values of the OFC model emulating the aging effect. B. Left column gives the velocity range reported in the RK-diagram. Right column gives the ΔF-values mentioned in the rule 4' to emulate the relative velocity between the plates of the OFC

A. Age (Myr)	**γ-values**
20	0.200
30	0.190
40	0.180
50	0.170
60	0.160
70	0.150
80	0.140
90	0.130
100	0.120
110	0.110
120	0.100
130	0.090
140	0.080
150	0.070

B. Velocity (cm/yr)	**ΔF-values**
1	0.25
2	0.5
3	0.75
4	1
5	1.25
6	1.5
7	1.75
8	2
9	2.25
10	2.5
11	2.75
12	3

In Fig. 1 we present the RK diagram in a version taken from Lay and Wallace [4]. In this figure we can see that in the upper right of the RK-diagram; that is, in the zone of high convergence rates and young lithospheric plates, the largest earthquakes are registered (e.g. $M_w 9.5 Chile 1960$). On the other hand, in the zone of low convergence rate and old lithospheric plates the smallest characteristic earthquakes are observed (e.g. $M_w 7.2 Marianas 1931$). If we use the synthetic data reported in column 2 of Table 1A and in column 2 of Table 1B, we can elaborate an equivalent figure to the RK diagram. In Figs. 1 and 2 we observe that evidently does not exist a formal relationship between the actual convergence rates and the relative synthetic "velocities" and neither between the age of the tectonic plates and the aging effect described by the γ-elastic ratios. As a matter of fact, the unique relationship between such variables is of qualitative nature. However, if we incorporate to the OFC model a quantity to measure the magnitude of the synthetic earthquakes, through $M = log_x n$, where n is the number of relaxed blocks and x is a convenient base of the logarithm, then an utilitary (toy model-type) comparison between both diagrams, the actual RK-diagram and a kind of synthetic RK-diagram is possible. What Ruff and Kanamori discovered was that M_w is correlated through a bilinear relationship (see Fig. 11.34 of [4] and Fig. 4 of this article) with the two variables convergence rate between tectonic plates and with the age of the corresponding subducting oceanic lithosphere respectively. It is very interesting that within the OFC SOC synthetic context a kind of RK-diagram exists and in addition a bilinear relationship also exists (see Fig. 5). In Figs. 2 and 4 the synthetic magnitude was estimated natural logarithms of the number of relaxed blocks, the extreme values of the magnitudes of the synthetic

earthquakes considered in the RK-type synthetic diagram (Fig. 4) are very close to the largest characteristic earthquakes located within the actual RK-diagram.

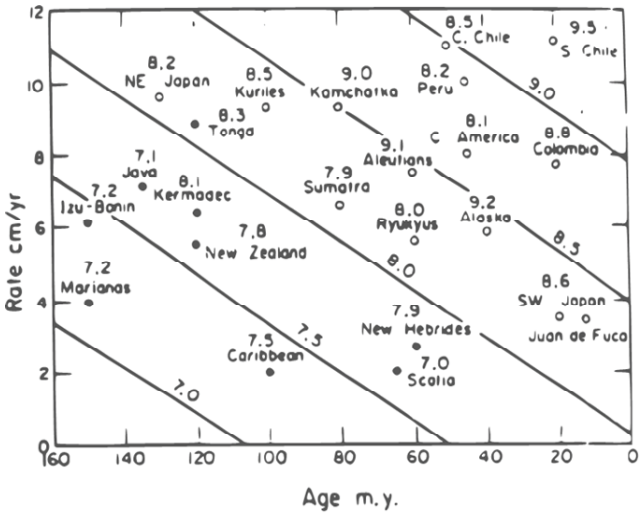

Fig. 1 – Ruff-Kanamori diagram taken from Lay and Wallace [4]

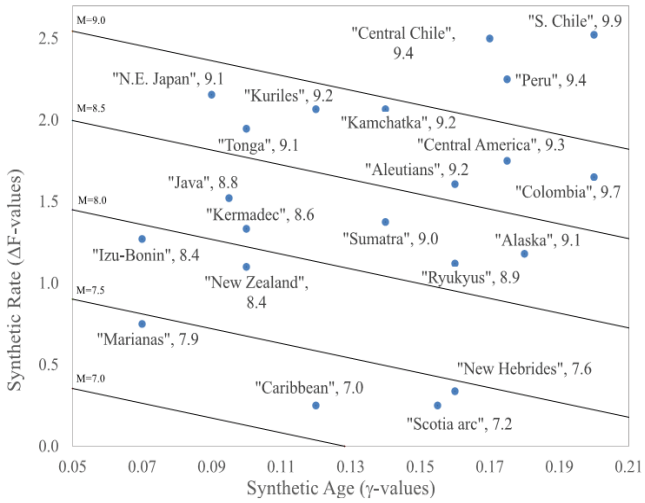

Fig. 2 – Synthetic Ruff-Kanamori diagram (adapted from [11])

The extreme magnitudes in the RK-diagram are $M_w 9.5 SChile 1960$ and $M_w 7.0 ScotiaArc 1924$, and when we calculate $M_{syn} = ln(n)$, the role of the largest earthquake located at the upper right zone of the RK-diagram; that is, the $M_w 9.5 SChile 1960$ is played by $M_{syn} = ln(20863) = 9.946$ for the RK-type synthetic diagram. On the other hand, for the other extreme in the down left of the actual RK-diagram; that is, $M_w 7.0 ScotiaArc 1924$, the corresponding role in the synthetic RK-diagram is played by $M_{syn} = ln(1399) = 7.243$. For the rest of the regions of the RK-diagram the difference between the actual M_w

magnitudes and the synthetic magnitudes present no dramatic variations for most of the cases (only in 25% of the cases the percent error was larger than 10% and less than 24%.

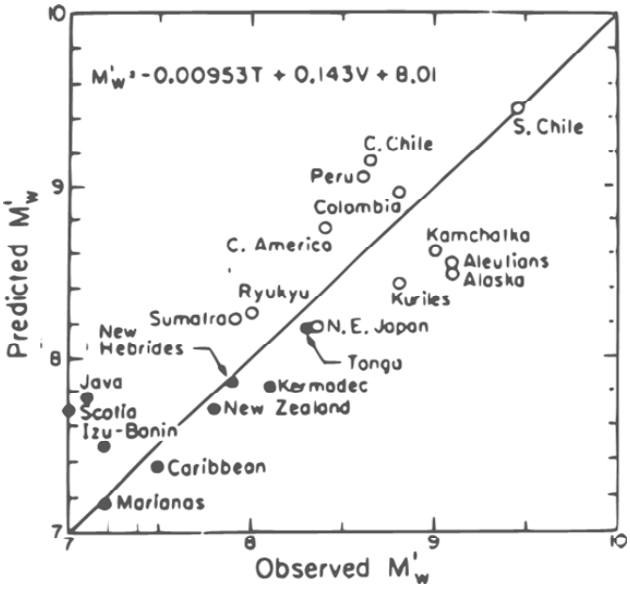

Fig. 3 – Linear multivariate fit for seismic zones of the Ruff-Kanamori diagram. Taken from reference [4]

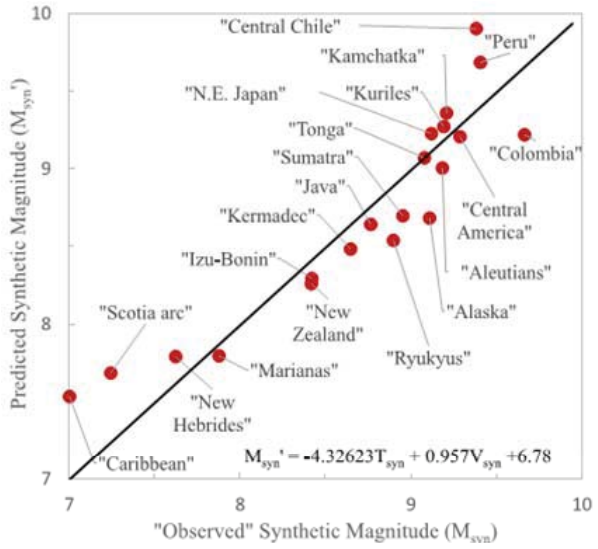

Fig. 4 – Linear multivariate fit for synthetic "seismic zones" of the Synthetic RK diagram (adapted from reference {11])

In the RK diagram one can observe that Marianas seismic zone has an age of around 150 millions of years and that its maximum earthquake is $M_{\max} = 7.2$ and on the other hand, the Chilean trench has an age of around 20 millions of years and with $M_{\max} = 9.5$. That is, the younger the tectonic zone the greater the maximum magnitude of their characteristic earthquake and the older the tectonic zone the smaller the

maximum magnitude of their characteristic earthquake. Evidently, the Chilean trench corresponds to the first case and Marianas corresponds to the second case.

From reference [4] the data contained in the RK-diagram were taken to calculate a linear multivariate fit to obtain an expression for M_{w_p} resulting in

$$M_{w_p} = -0.00953T + 0.143V + 8.01, \quad (3)$$

where the subindex p means predicted; T is the age of the tectonic plate and V is the relative velocity between downgoing and upper plates. In Fig. 3 a comparison between the calculated M_{w_p} and the actual M_w is shown, one can see that both values reasonably agree. From Eq. (3) an anticorrelation between the magnitude M_w and the age of the tectonic plate T is evident for a constant velocity V. In Section 3 we explain how we construct a synthetic RK-diagram. Following the same procedure used by Lay and Wallace [4] to calculate Eq. (3) but using the synthetic data of Fig.2 to obtain a linear multivariate fit (see Fig. 4), we get,

$$M_{syn_p} = -4.326T_{syn} + 0.957V_{syn} + 6.776 \quad (4)$$

As we said for Eq. (3), if V is constant an anticorrelation arises between M_w and T. The same occurs for Eq. (4), if V_{syn} is constant then a similar behavior between M_{syn} and the γ elastic ratio is observed where γ plays the inverse role of T in actual seismicity. When we plot M_{syn_p} given by Eq. (4) against M_{syn} as given in the synthetic RK-diagram of Fig. 2, stemming from the practical definition $M_{syn} = ln(n)$, we can see in Fig. 4 that the agreement between M_{syn_p} and M_{syn} is very good.

4. Conclusions

Many researchers have proposed numerical models that reproduce some important features of actual seismicity by using suitable simplified SOC models capturing the main dynamical characteristics of earthquakes. However, the SOC nature of the seismicity would be reinforced if other of its important characteristics were also reproduced by these models. One of our goals was to reproduce the so-called Ruff-Kanamori diagram, which relates the magnitude (M_w) of the largest characteristic earthquake of a given subduction zone with the convergence rate between the downgoing and upper plates and with the age of the subducted plate. On the other hand, the convergence rate in the RK diagram was emulated adding a new rule (rule 4') to the set of rules of the OFC model. Interestingly, we obtained that M_{syn} depends on the synthetic velocity and the synthetic age by means of Eq. (4) which is qualitatively equivalent to Eq. (3) describing properties of actual seismicity.

5. Acknowledgements

AMD and FAB thank the partial support from COFAA-IPN and EDI-IPN and JPO thanks support from CONACYT-México.

6. References

References must be cited in the text in square brackets [1, 2], numbered according to the order in which they appear in the text, and listed at the end of the manuscript in a section called References, in the following format:

[1] Gutenberg B, Richter CF (1944): Frequency of earthquakes in California. *Bulletin of the Seismological Society of America*, **34**(4), 185–188.

[2] Gutenberg R, Richter CF (1954): Seismicity of the Earth and Associated Phenomena. Princeton, New Jersey: Princeton University Press.

[3] Ruff L, Kanamori H. (1980): Seismicity and the subduction process. *Physics of the Earth and Planetary Interiors* **23**(3), 240-252.

[4] Lay T, Wallace TC (1995): *Modern global seismology*. Elsevier.

[5] Olami Z, Feder HJS, Christensen K (1992): Self-organized criticality in a continuous, nonconservative cellular automaton modeling earthquakes. *Physical Review Letters*, **68**(8), 1244.

[6] Christensen K, Olami Z (1992): Variation of the Gutenberg-Richter b values and nontrivial temporal correlations in a Spring-Block Model for earthquakes. *Journal of Geophysical Research: Solid Earth*, **97**(B6), 8729–8735.

[7] Ferguson CD, Klein W, Rundle JB, Gould H, Tobochnik J (1998): Long-range earthquake fault models. *Computers in Physics*, **12**(1), 34–40.

[8] Angulo-Brown F, Muñoz-Diosdado A (1999): Further seismic properties of a spring-block earthquake model. *Geophysical Journal International*, **139**(2), 410–418.

[9] Muñoz-Diosdado A, Rudolf-Navarro AH, Angulo-Brown F. (2012): Simulation and properties of a non-homogeneous spring-block earthquake model with asperities. *Acta Geophysica*, **60**(3), 740–757.

[10] Perez-Oregon J, Muñoz-Diosdado A, Rudolf-Navarro AH, Guzmán-Sáenz A, Angulo-Brown F (2018): On the possible correlation between the Gutenberg-Richter parameters of the frequency-magnitude relationship. *Journal of Seismology*, **22**(4), 1025-1035.

[11] Perez-Oregon J, Muñoz-Diosdado A, Rudolf-Navarro AH, Angulo-Brown F (2019): Some common features between a spring-block self-organized critical model, stick-slip experiments with sandpapers and actual seismicity. *Pure and Applied Geophysics* doi.org/10.1007/s00024-019-02320-2.

[12] Pardo M, Suárez G (1994): Shape of the subducted Rivera and Cocos plates in southern Mexico: Seismic and tectonic implications. *Journal of Geophysical Research Atmospheres* **1001**(B7), 12357-12374.

